
DESIGN AND IMPLEMENTATION OF A DUAL UNCREWED SURFACE VESSEL PLATFORM FOR BATHYMETRY RESEARCH UNDER HIGH-FLOW CONDITIONS

Dinesh Kumar, Amin Ghorbanpour, Kin Yen, Iman Soltani*

Department of Mechanical and Aerospace Engineering

University of California, Davis, CA 95616

*isoltani@ucdavis.edu

ABSTRACT

Bathymetry, the study of underwater depth and topography, relies on detailed sonar mapping of the underwater structures. These measurements, critical for infrastructure health monitoring and hazard detection, often require prohibitively expensive sensory equipment and stable measurement conditions. The high financial risk associated with sensor damage or vessel loss creates a reluctance to deploy uncrewed surface vessels (USVs) for bathymetry. However, the alternative, crewed-boat bathymetry operations, are costly, pose significant hazards to personnel, and frequently fail to achieve the highly stable conditions necessary for bathymetry data collection, especially under challenging conditions such as high currents. Consequently, further research is essential to advance autonomous control, navigation, and data processing technologies, with a particular focus on bathymetry while ensuring safety under extreme conditions. There is a notable lack of accessible hardware platforms that allow for integrated research in both bathymetry-focused autonomous control and navigation, as well as data evaluation and processing. This paper addresses this gap by detailing the design and implementation of two complementary (dual) research USV systems tailored for uncrewed bathymetry research. This includes a low-cost USV for Navigation And Control research (NAC-USV) and a second, high-end USV equipped with a high-resolution multi-beam sonar and the associated hardware for Bathymetry data quality Evaluation and Post-processing research (BEP-USV). The NAC-USV facilitates the investigation of autonomous, fail-safe navigation and control technologies, emphasizing the stability requirements for high-quality bathymetry data collection while minimizing the risk to expensive equipment, allowing for seamless transfer of validated controls to the BEP-USV. The BEP-USV, which mirrors the NAC-USV hardware, is then used for additional control validation and in-depth exploration of bathymetry data evaluation and post-processing methodologies. We detail the design and implementation of both USV systems, open source hardware and software design, and the bill of material. Furthermore, we demonstrate the system's effectiveness in both research and bathymetric applications across a range of operational scenarios.

Keywords Autonomous systems · Bathymetry · Maritime engineering · ArduPilot · Uncrewed · Surface Vessels (USV) · Underwater surveying

1 Introduction

Bathymetry, the study of underwater depth and topography, is essential for numerous applications, including infrastructure health monitoring [1], preventive maintenance [2], navigation safety [3], underwater archaeology [4], and scouring evaluation [5] to name a few. Some applications related to underwater engineering [6], marine sciences [7], archaeology [8], and defense [9] require high-resolution bathymetric surveys.

A safety critical example application of bathymetry is related to the inspection of underwater infrastructure, particularly bridges [10, 11, 1]. This involves assessing the structural integrity and safety of submerged infrastructure such as bridge foundations, pipelines, and cables. Such inspections are vital for identifying potential issues that could lead to

catastrophic failures. For underwater infrastructure as an example, regular bathymetry inspections seek to detect signs of damage or deterioration including scour (the erosion of sediment caused by flowing water around bridge foundations), as well as cracks, corrosion, and deformation. Scour, particularly, poses a substantial threat by potentially undermining structural stability and leading to disastrous bridge collapses if unaddressed (Fig. 1). A notable incident underscoring the importance of frequent bathymetry was the collapse of the Schoharie Creek Bridge in New York in 1987, which resulted in ten fatalities [12]. This collapse was triggered by severe scour due to snow melting and record rainfall that quickly eroded the sediment beneath a bridge pier.

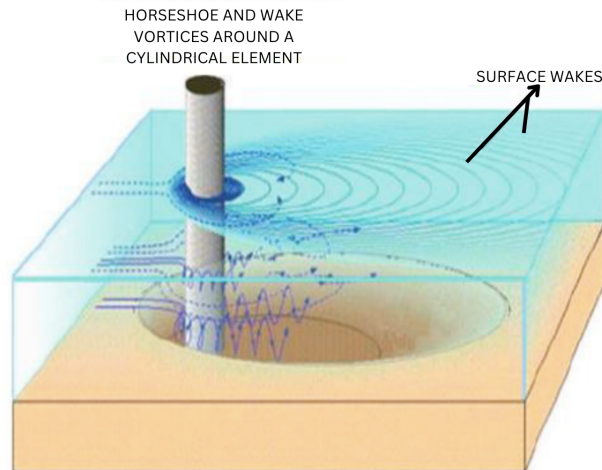


Figure 1: Scour holes around a bridge pier [13].

High-precision surveys required in such safety-critical applications necessitate sophisticated sensory equipment, which can be prohibitively expensive. These systems include MultiBeam EchoSounders (MBES) that emit thousands of sound pulses per second across a wide area of the sea/riverbed and capture their echoes. They further include Differential GPS (DGPS) or Real-Time Kinematic (RTK) GPS as well as high precision IMU to allow for subsequent high-precision registration of measurements. The financial risk associated with potential damage or loss of the bathymetry equipment often creates a tendency to adopt crewed operations, despite the associated hazards, discomfort, labor intensity, and corresponding costs, ultimately compromising the frequency and quality of data collection. Additionally, many locations with elevated scouring risk, such as river narrowing under bridges, feature persistent high flow conditions, increasing the risk to human operators and complicating the acquisition of reliable data that is free of motion artifacts. Given these challenges, there is a critical need to advance research and development of robust, fail-safe bathymetry USV systems designed to collect high-quality data in diverse and demanding environments, including areas with high-flow conditions.

The first step for research in automated bathymetry is the development of hardware platforms that allow for safe evaluation of new techniques for bathymetry USV navigational and functional robustness as well as high quality data collection and processing under real-world conditions without excessive concerns about the potential risks to equipment. Such a research platform must be equipped with fail-safe mechanisms to prevent unpredictable or risky actions that could compromise hardware, yet still offer researchers the freedom to explore novel control, instrumentation, machine learning and design approaches. This balance is inherently challenging, as the flexibility required for experimental research often conflicts with the need for strict monitoring and constraints that enhance safety. Currently, there is a gap in the availability of such research platforms that can meet these conflicting requirements. This paper aims to bridge this gap by detailing the design and implementation of a dual-USV platform specifically tailored for bathymetry research.

To be universally applicable, bathymetric measurements must adhere to established hydrographic standards. This includes ensuring that data collection and processing methodologies, as well as survey accuracy, are in alignment with international standards such as the IHO S-44 Special Order [14]. The quality of data is affected by several factors, including the motion of the system hosting the sonar [14]. Bathymetric surveys conducted in challenging environments—ranging from coastal regions to flood scenarios and areas with persistent high flow conditions, such as river narrowing under bridges—often experience vessel motions. In conditions with high winds and waves, due to the induced movements, small inaccuracies in calibration and registration of sensors can lead to large accumulated errors including inaccurate measurements of depth[15]. Due to USVs' smaller mass when compared to crewed vessels, these effects may be more pronounced, thus adding to the challenges of data collection. [14] highlights how the motion of USVs in different sea states can drastically impact data quality, showing a marked decline in data reliability at early sea

state 3 (characterized by waves around 3 feet high and wind speed of 14 knots [16]). Ship-based surveys, with their larger mass and higher inertia, can typically operate in late sea states 3 (characterized by waves around 6 feet high, and wind speeds of 18 knots[16]) before data quality becomes compromised. While post-processing motion compensation techniques are adopted in advanced bathymetric systems, their effectiveness drops as vessel movements increase. These methods further face limitations caused by water clarity, surface currents, limited scan range and finally excessive cost [15].

As such, robust and stable bathymetry-USV navigation and control, is of critical importance. Advanced solutions, such as machine learning (ML)-based path planning and control, hold promise against environmental disturbances, as similar approaches have proven successful in UAV systems for gust rejection [17, 18, 19]. Some progress has already been made in this area [20, 21], but the developed methods are often tailored to specific marine conditions, limiting their generalizability. Expanding these solutions to create adaptive, environment-agnostic control systems could greatly enhance the operational flexibility of USVs in bathymetric surveys. Furthermore, the high cost of MBES sensors (in the order of hundreds of thousands of dollars) and USVs necessitates stringent safety measures to prevent platform loss, and sensor damage and also avoid potential harm to other vessels and personnel. Ensuring operational safety is critical, especially in adverse environmental conditions where control and stability are challenged. Novel control schemes that provide both safety and performance guarantees under such conditions are essential for the broader adoption of these systems. Although advances in collision avoidance and disturbance handling have been achieved in USVs [22, 23, 24] direct application to bathymetric USVs remains difficult due to the unique operational challenges and specific performance requirements of these vessels.

In any case, regardless of the applied navigation and control techniques, residual motion artifacts will inevitably persist in the data. Thus, post-processing of data is considered another crucial step in hydroacoustic measurements [16]. The complexity and nuances of post-processing schemes are heavily influenced by the challenges and limitations of USV control. Therefore, post-processing must be dynamically integrated with control strategies, calling for a concurrent investigation of both vessel control and data processing techniques, ensuring that advancements in one area can inform and enhance the other. However, many of the state-of-the-art data processing techniques have been adopted from other domains with no consideration of the unique characteristics of bathymetric data. As an example, due to nearly flat seabed topography, the occurrence of invalid loop closures is unavoidable in bathymetric SLAM [25]. Furthermore, continuous environmental disturbances make USVs particularly prone to exacerbated drifts in dead reckoning, resulting in degraded resolution of MBES data [26]. This is of additional concern when dealing with GPS signal loss, which is common below overpasses and near bridge columns. In bathymetry, small IMU drift can lead to large errors, rendering the data unusable. Although, utilizing higher-grade IMUs, such as those compliant with MIL-STD 810 or MIL-STD 461, can be helpful [27], they significantly increase the cost of the platform and still suffer from limitations. In recent years, the research emphasis on bathymetry-specific data processing has predominantly been on relatively simple steps such as improvements in data acquisition [28] and data cleaning methods [29]. Consequently, despite its critical importance, bathymetry data post-processing remains a relatively under-explored area [30]. Much like navigation and control, bathymetry post-processing stands to benefit from recent advancements in machine learning. Studies such as [26] explore deep-learning methods for loop closure in underwater bathymetry mapping, but these efforts remain limited and warrant further expansion. Given the direct effect of GNC (Guidance, Navigation, Control) performance on bathymetry data post-processing challenges and requirements, tackling both GNC and post-processing aspects simultaneously could significantly accelerate progress in this field.

The first step toward addressing these research challenges is to facilitate access to research hardware platforms that enable experimentation. Currently, there are limited resources available to researchers for developing USV platforms tailored to bathymetry and related GNC research. To the best of our knowledge, there is no open-source research platform that allows for simultaneous investigation of GNC and data processing with a focus on bathymetric applications. Various research papers document the development of USV platforms—covering control system design, mechanical structure, and GNC algorithms in a limited and isolated fashion [31, 32, 33, 34]. Hence, there is a need for a comprehensive hardware and software setup that supports research in this domain. This work seeks to bridge this gap by introducing a fully open-source research platform.

We introduce implementation details of a dual-USV system, designed for autonomous bathymetry research. Our platform comprises an NAC-USV and a BEP-USV system, engineered to operate across a spectrum of safety and flexibility settings. The NAC-USV facilitates navigation and control development and testing, offering capabilities ranging from direct propeller control to high-level navigation including position and speed/heading control. The BEP-USV facilitates the implementation and further evaluation of methods tested on the NAC-USV, with additional focus on bathymetry-specific requirements under more extreme environmental conditions. The BEP-USV also serves as a platform for investigating techniques to evaluate and process bathymetry data collected under real-world conditions. By separating the NAC and BEP platforms while maintaining identical hardware specifications and implementation requirements, we mitigate concerns about safety, thereby removing barriers to flexible research.

This paper provides detailed descriptions of the hardware and software implementations for both USV systems, lists all components, and shares the CAD models and software publicly to encourage transparency and collaboration within the research community. The structure of this paper is organized as follows: Section 2 outlines the bathymetry mission requirements. Section 3 explores the mechanical design of the dual-USV system, including methodologies for drag and thruster calculations. Details of the mechanical and electrical hardware implementations are covered in Sections 4 and 5, respectively. Section 6 describes the control strategies employed in the dual-USV system. Finally, Sections 7 and 8 present the experimental results and conclusions, respectively.

2 Mission Requirement

The primary objective of the BEP-USV platform discussed herein is to conduct bathymetry surveys in diverse environments, including high-current conditions. This requirement is crucial, particularly in areas like those near bridges, where frequent bathymetric surveys are necessary due to strong currents and limited access, presenting significant operational challenges. To fulfill its mission objectives, the USV must meet several critical performance requirements. These include the capability to reach speeds approaching 7 knots, enabling operation under high flow conditions. The system must also have sufficient battery capacity to operate continuously for at least one hour, ensuring comprehensive data collection in a single deployment. In addition, given the required instrumentation including multi-beam sensor, onboard computational resources and battery support, the boat should also have a payload capacity of at least 50 lbs. Given the extremely high cost of the onboard equipment, the bathymetry survey must be executed safely, minimizing the risk of damage or loss. As such, it is crucial to conduct numerous tests during the research phase to ensure of fail-safe performance of the USV under targeted extreme conditions. This necessity underscores the need for research flexibility as well as implementation robustness, two inherently competing attributes. For this purpose, we propose the adoption of a secondary USV system, NAC-USV, which features similar specifications as those of the BEP-USV but is significantly less expensive and relatively easy to set up. Its primary purpose is to evaluate the hardware and navigation/control software under various conditions before deployment on the BEP-USV which then allows for further research with more emphasis on the final task of bathymetry data collection and analysis. The BEP-USV and the NAC-USV setups are shown in Figs. 2 and 3.

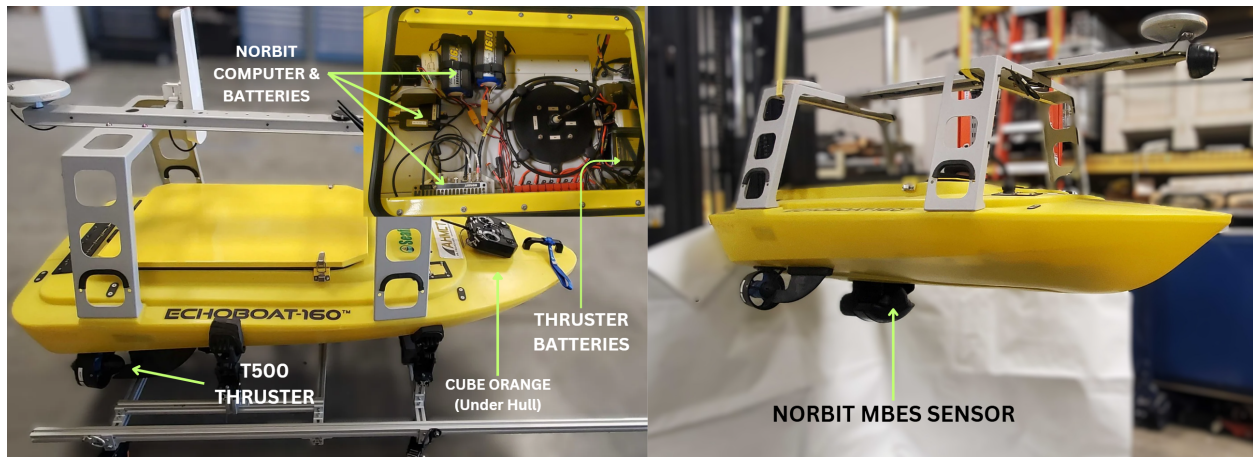


Figure 2: The BEP-USV.

In the following, we discuss our design approach and implementation details. The design discussions apply to both boats and are not specific to either unless explicitly stated otherwise. It's important to note that the outlined requirements can be competing; for instance, enhancing payload capacity adversely affects both speed and endurance, making the design an iterative process. In the following, we discuss the mechanical design process in detail.

3 Mechanical design

We employ an iterative design process, beginning with the selection of a hull best suited to meet the initial design specifications. This is followed by detailed drag calculations to assess hydrodynamic resistance at the desired speed for the selected hull, which informs our estimates of the required thrust. The thrust estimate then guides our thruster selection. If the design proves unfeasible—for instance, if the thrust estimate is excessively high—we refine the process, starting again with hull selection and continuing until all criteria are met.

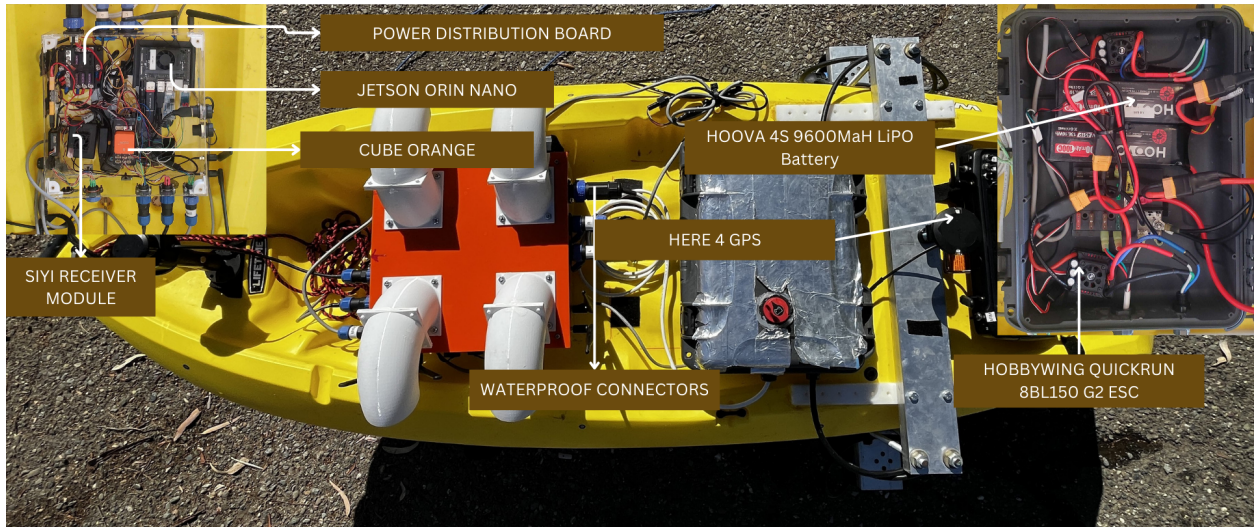


Figure 3: The NAC-USV.

3.1 Hull selection

The hull of the USV serves as its physical framework, providing structural integrity and buoyancy. It is typically made of durable, light-weight materials such as carbon fiber [35]. The hull profile, directly tied to USV hydrodynamics, plays a crucial role in the USV's stability, speed, maneuverability, and robustness to diverse environmental conditions [35]. Additionally, the hull is responsible to house and protect the internal components of the USV, such as the electronics.

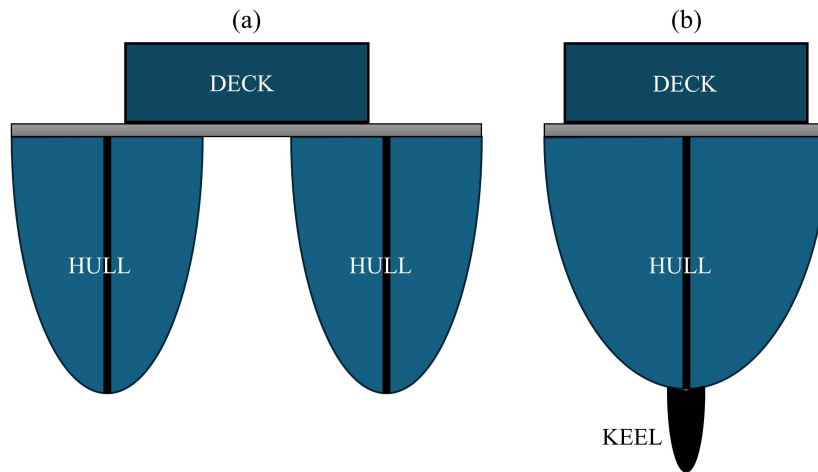


Figure 4: Types of USVs. (a) Catamaran, (b) Monohull

There are two choices for the USV body design: catamarans and monohulls, as shown in Fig. 4. Unlike a monohull, a catamaran features a twin-hull design connected by a deck, which can potentially offer superior roll stability [35]. However, the deck space connecting the hulls is often used to house components like electronics, leading to challenges in evenly distributing the weight. This can hinder the full realization of the catamaran's inherent stability advantage. Monohulls, on the other hand, are easier to maneuver in tight spaces and often excel at upstream navigation thanks to their deep keel design [35]. Its superior maneuverability in tight spaces, for example near areas with vegetation, or near bridges where access is limited, is an important advantage. Additionally, the monohull's structure provides a simpler setup by allowing for easier integration and protection of all equipment inside the hull, reducing the need for extra wiring, and providing more flexibility in setting the center of gravity for stability purposes [?, 35]. They are also typically less expensive in terms of fabrication and maintenance compared to catamarans. As such, a monohull seems to be the better choice for bathymetry.

The hull shape also affects the stability, drag, and overall performance of a USV. Common hull shapes used for USVs include round-, rectangular-, V-shape-, and stepped-bottom designs [36] as shown in Fig. 5. Choosing the appropriate hull shape depends on the specific requirements of the USV, including its intended use, operational environment, and performance goals. Each shape offers distinct advantages and trade-offs in terms of stability, drag, manufacturability, and overall efficiency [37], [36]:

1. **Round:** Round hulls provide good buoyancy and stability and offer low drag at low speed and in calm waters. However, they may experience higher drag at high speeds and in rough waters, which can impact performance.
2. **Rectangular:** Rectangular hulls offer excellent stability and a large surface area for mounting equipment. However, they have higher drag compared to cylindrical and hydrodynamic shapes, making them less efficient in terms of speed.
3. **V-shape:** V-shaped hulls exhibit lower drag compared to rectangular and round hulls, and also provide good stability, especially at higher speeds. The main drawback is their complex manufacturing process, potentially increasing production costs.
4. **Stepped:** Stepped hulls feature one or more horizontal steps along the bottom of the hull, which reduce drag and enhance performance at higher speeds. These steps also improve the boat's wave-piercing abilities, making them suitable for rougher waters. The manufacturing process for stepped hulls is challenging and costly.

Among hull designs, V-shaped and stepped hulls are most commonly chosen for high-speed operations. The V-shaped hull is the most appropriate choice for our application as it offers an optimal balance of speed, stability, and performance [38].

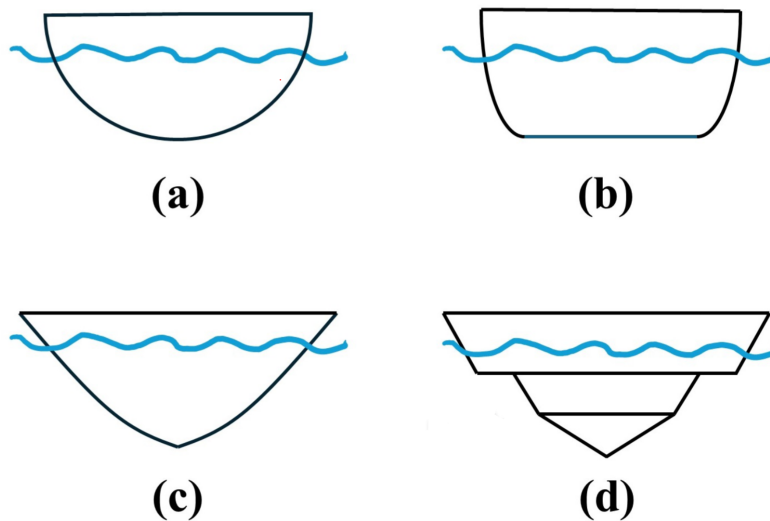


Figure 5: Common types of bottom hull design, a) round, b) rectangular, c) V-shape, d) stepped.

3.2 Estimation of Total Hull Resistance

To meet the maximum speed requirement, it is essential to accurately estimate the required thrust. However, this estimation must be preceded by determining the drag force associated with the selected hull, as it directly influences the thrust needed for the desired speed. In this section, we calculate the total hull resistance, R_T , which is a function of several parameters, including ship speed, hull geometry - such as draft - vertical distance between waterline to bottom of vessel's hull, beam - widest part of vessel, wetted surface area - surface area in contact with water, length, as well as water density and kinematic viscosity. The main components contributing to the total USV resistance are the fluid friction/viscous drag (R_V), wave drag (R_W) and air (R_A) resistance. The total resistance is written as [39, 40], $R_T = R_V + R_W + R_A$.

R_A can be neglected ($R_A \approx 0$) since its contribution is only significant for large sizes, extremely high ground speeds, or strong wind conditions, which can largely be avoided in this application. Hence,

$$R_T = R_V + R_W \quad (1)$$

1) **Viscous Drag:** The viscous drag, R_V , increases with speed as shown in Fig. 6. It is caused by the friction and pressure forces on the hull due to the USV motion. Based on the assumption of a flat plate geometry for the hull, corrected for form factor as outlined in [40], the viscous drag can be approximated as:

$$R_V = \frac{1}{2} \rho V^2 C_F (1 + K) S_{wet} \quad (2)$$

where, C_F is the friction coefficient (Eq. 3 [41]). The form factor K (Eq. 4 [40]) accounts for the effect of hull geometry on viscous resistance. The wet surface area, S_{wet} , quantifies the submerged surface area (Eq. 5 [40]). We have:

$$C_F = \frac{0.075}{((\log_{10} R_n) - 2)^2} \quad (3)$$

$$K \approx 19 \left(\frac{\nabla}{L^2 \times D} \right)^2 \quad (4)$$

$$S_{wet} = 2 \times (L \times B + B \times D + L \times D) \quad (5)$$

where L, B, D, ρ, V denote the length, breadth, draft, fluid density and speed of the USV, respectively. $R_n = LV/\nu$ is the Reynolds number, and ν is the kinematic viscosity of fluid. ∇ is the volume of fluid displaced by the boat.

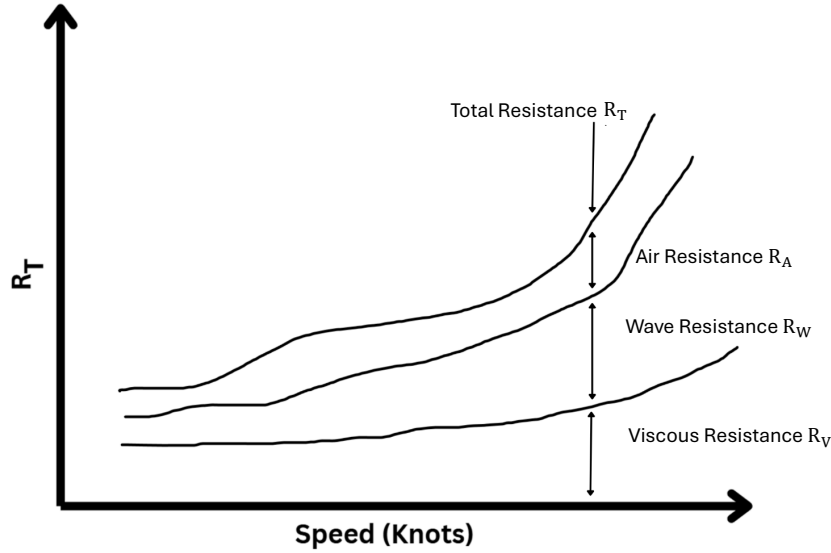


Figure 6: Viscous, wave, and air resistance are the key factors contributing to the total resistance encountered by a vessel moving through water [40].

2) **Wave Drag:** At higher velocities, wave drag may form a significant portion of the total drag as observed in Fig. 6. Naval architects use the dimensionless Froude number, defined below, to predict the significance of wave drag [40]:

$$F_n = \frac{V}{\sqrt{gL}} \quad (6)$$

where g is the gravitational acceleration. It is shown that for small Froude numbers, $F_n < 0.3$, the USV's movement does not generate significant waves, and hence, the wave drag can be neglected [40]. For Froude numbers, $F_n > 0.5$ wave drag accounts for a significant part of the generated drag [40].

Estimating wave drag is challenging, as it requires complex experimental or numerical studies. [41] performed multiple resistance measurements on different vessels, and formulated a model for wave drag estimation:

$$R_W = \Delta \cdot c \cdot e^{m_1 F_n^{-0.9} + m_2 \cos(\lambda F_n^{-2})} \quad (7)$$

where Δ is mass displacement ($\nabla \times \rho_{water}$). In this work, the model parameters c , m_1 , m_2 , λ are calculated per [41]:

$$c = 569 \cdot \left(\frac{B}{L}\right)^{2.984} \cdot C_M^{-0.7439} \cdot C_{WL}^{1.2655}$$

$$m_1 = -4.8507 \cdot \frac{B}{L} - 8.1768 C_p + 14.034 C_p^2 - 7.0682 C_p^3$$

$$m_2 = -0.4468 \cdot e^{-0.1 F_n^{-2}}$$

$$\lambda = 1.446 \cdot C_p - 0.03 \cdot \frac{L}{B}$$

where C_p , C_M , and C_{WL} are dimensionless coefficients commonly used to characterize and compare marine vessels. For additional details, readers are encouraged to refer to [42]. These coefficients are calculated as follows:

$$C_p = \frac{\nabla}{A_M \cdot L} \quad (8)$$

$$C_M = \frac{A_M}{B \cdot D} \quad (9)$$

$$C_{WP} = \frac{A_{WP}}{L \cdot B} \quad (10)$$

In Eqs. 8, and 9, A_M denotes the submerged midsection area of the boat [42], as illustrated in Fig. 7. Similarly, in Eq. 10, A_{WP} represents the surface area of the top-down view of hull at the waterline, as shown in Fig. 8.

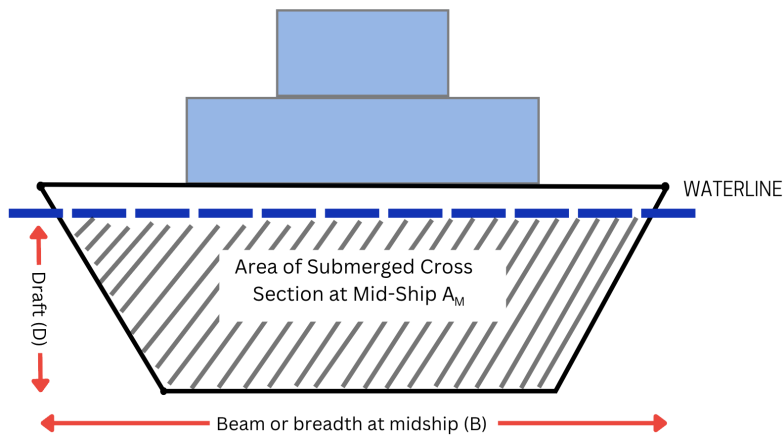


Figure 7: Area of submerged cross-section at midship (A_M) used to calculate the prismatic coefficient (C_p) [42].

Given R_V (Eq. 2), and R_W (Eq. 7), the total resistance (Eq. 1) can be calculated.

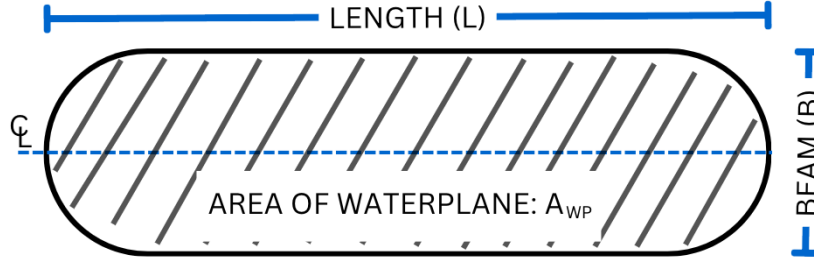


Figure 8: Area of Waterplane (A_{WP}) used to calculate the waterplane coefficient (C_{WP}) [42].

3.3 Propulsion Mechanism

Thrusters generate propulsion and steering, with propeller-based systems—such as open and jet propellers—being the most popular due to their versatility. For the bathymetry mission, open propellers are preferred over jet propellers due to their superior efficiency across a wide range of speeds and conditions [43]. They are also more cost-effective in terms of maintenance and occupy less space. Finally, unlike jet propulsion, open propellers can easily provide forward and reverse movements without the need for special mechanisms.

Depending on the desired steering mechanism, open propellers can be incorporated into a USV in various ways, including differential thrust, rudder-based systems (such as twin-screw setups), and vectored thrust. Differential thrust relies on thrust resultant and thrust imbalance across two or more propellers to respectively propel and maneuver the USV. This method eliminates the need for a rudder and allows for more effective control, especially for small to medium-sized vessels [44]. A twin-screw configuration includes one rudder behind each propeller. This setup is commonly used in larger vessels. In a vectored thrust system, the thrusters can rotate and change the direction of the resultant thrust force, enabling the USV to move forward, backward, and laterally, and also make sharp turns. This setup provides exceptional maneuverability, making it ideal for complex navigational tasks, although with additional complexity. Among these three steering methods, differential thrust presents a good trade-off between simplicity and performance and achieves acceptable maneuverability in most environmental conditions [45]. Hence, it is selected for our USV system.

3.4 Estimation of the Required Thrust

The first step in estimating the required active thrust, T_a , is to determine the total hull resistance, R_T , as was discussed in section 3.2. At a constant speed, the active thrust is equal to the total hull resistance, i.e. $T_a = R_T$. One also needs to account for moving thrust efficiency, $\eta_e < 1$, defined as the ratio between the active and the nominal propeller thrust $\eta_e = T_a/T_n$. Therefore, the nominal thrust of the propulsion system is higher:

$$T_n = \frac{T_a}{\eta_e}$$

η_e is often provided in the data sheets of off-the-shelf propellers. η_e is typically, $0.15 < \eta_e < 0.7$ [46].

Following the estimation of the required nominal thrust, T_n , including a safety margin, k_s , is advisable to account for the uncertainty of external factors, such as unexpected extra thrust requirements during aggressive maneuvering for collision avoidance or in adverse environmental conditions, e.g., when encountering stronger than expected currents or winds. The final estimate of the required thrust, $T_f = k_s T_n$, can inform the sizing and number of the propellers.

4 Mechanical hardware implementation

Following the design process discussed earlier, in the following we go through each step and explain the implementation details for both BEP and NAC USVs.

4.1 BEP-USV

We examined several commercial off-the-shelf (COTS) boats. Our evaluation criteria included maximum achievable top speed, maximum payload, and compatibility with commercially available propulsion systems. Additionally, we paid

close attention to the equipment bay, giving priority to those specifically designed to reliably house critical components such as sensors, batteries, control systems, communication devices, and other necessary hardware for bathymetry USV’s operation. Finally, to ensure the boat is easily portable for deployment, we limited the overall USV length to under 2 meters, making it compatible with a standard-bed pickup truck in the United States [47]. In case manual transportation is needed in any stage of the deployment, assuming the involvement of 2-3 operators, based on single person max load of 51lbs (23Kgs) [48], we attempt to keep the overall weight (Hull weight + payload) near or below 70 kg. Keeping the overall weight low also reduces the risk to other boats and individuals in case of collision.

The heaviest part of the payload in a bathymetry boat corresponds to the multibeam sensor and the batteries. Adding other necessary electronics and processing/communication hardware, we estimated an upper limit of 30 kg for our total payload. Taking into account the high flow rates typically observed in Sacramento and other California rivers—such as the American River at Chili Bar and North Fork Dam, where water velocities range from 3 to 5 knots [49], along with the standard bathymetry survey speeds of 2–5 knots [50]—a maximum operational speed of 7 knots (3.6 m/s) has been selected. This speed strikes an optimal balance between navigating strong currents and ensuring efficient data collection during surveys.

Following a thorough market search, we selected the Echoboat-160 from Seafloor Systems [51], as shown in Fig. 2. The Echoboat-160 has an empty weight of 50 kg and a maximum payload capacity of 27 kg. The boat comes with two T200 thrusters from Blue Robotics [52] and can achieve a top speed of 3 knots (for empty hull). The boat design allows replacing the thrusters to increase the maximum speed. As shown in Fig. 2 the USV features an enclosure for mounting additional equipment. Inside the equipment bay, there is a mounting plate designed for equipment installation, which sits on dampers to reduce vibration and enhance safety. The length (L), width (B) and height (H) of the boat hull are 1.7m, 0.8m, and 0.24m, respectively.

In the ship design literature, to accurately define the boat geometry, a multitude of parameters may be used to refer to distinct but oftentimes very similar quantities. For example, the length may be denoted as L_{WL} (length at waterline) and L_{BP} (length between perpendiculars). The width is often represented as B (beam) and with considerations of the waterline as B_{WL} (beam at waterline). Similarly, draft is denoted as T (draft) and T_{AVG} (average draft). For simplicity, we assume that each of these parameters can be represented with a single quantity and hence, use L , B , and D to represent length, width and draft, as provided by the boat manufacturer. Given the dimensions and geometry of the Echoboat-160, and the maximum allowed payload of 27 kg, we adopt the quantities listed in table 1 for drag and thrust estimation.

Table 1: USV Parameters

Parameter	Value
Max Velocity, V	7 knots = 3.6 m/s
USV Length, L	1.7 m
USV Width, B	0.8 m
Draft, D	0.25 m
Max Mass, M	77 kg
Midsection Area	0.231 m ²
Waterplane Area	1.075 m ²
Water Kinematic Viscosity, ν	1.002×10^{-6} m ² /s
Water Density, ρ	1000 kg/m ³
Volume Displacement, ∇	0.077 m ³

For the desired speed, per Eq. 6 the Froude number is $F_n = 0.85$. Hence, both wave and viscous drag will contribute to the total drag. Following the procedure discussed in section 3.2, we calculate the required coefficients, which are provided in table 2. The drag estimation results are summarized in table 3 indicating a total drag of $R_T = 215.23N$. Given the moving thruster efficiency of $\eta_e = 0.5$ (see section 5.0.4) we have $T_n = 430.46N$, and assuming a safety factor of $k_s = 1.25$, the final required thrust, $T_f = 538.07$.

Table 2: Coefficients and Parameters for Drag Estimation

Parameter	Value
Wet Surface Area	3.32 m ²
Reynolds Number, Re	5938123.75
Midship Section Coefficient, C_M	0.52
Prismatic Coefficient, C_P	0.17
Form Factor, K	0.9
Waterplane Area Coefficient, C_{WP}	0.7902
Friction Coefficient, C_F	0.00329126

Table 3: Estimated drag values

Parameter	Value
Viscous Drag, R_V	129.05 N
Wave Drag, R_W	86.18 N
Total Drag, R_T	215.23 N

4.2 NAC-USV

For the NAC-USV, our goal is to select a cost-effective, lightweight, and durable off-the-shelf small boat that is similar to the BEP-USV in terms of the hull shape and size. After reviewing the options available on the market, we opted for a generic kayak, widely available through various vendors at a low cost. The selected kayak (Lifetime Wave) measures 1.82m (L), 0.61m (W) and 0.2m (H), weighs 8.2 kilograms, and has a weight capacity of 59 kilograms. The dimensions match the BEP-USV and allow for considerable flexibility for installing electronics and adjusting mass distribution to align the center of mass with that of the BEP-USV. For any initial tests in the research phase of the control and navigation, the kayak may only carry essential electronics weighing approximately 12 kilograms i.e. for a total weight of nearly 20 kg. In this phase maintaining a low overall weight is essential to minimize the risk associated with potential collisions and loss of control. Following successful preliminary evaluations, the weight of the boat can be incrementally increased up to 67.2 kilograms using dummy masses to closely approximate that of the BEP-USV and extend control evaluations.

In the following, we discuss the electronics, control, and computing hardware, which are identical for the BEP and NAC USVs. Additional implementation details can be found on the GitHub page associated with this manuscript [53].

5 Electrical hardware Implementation

5.0.1 Power Source

There are several options available for the main power source of the USV, including Lithium Polymer (LiPo), Lithium-Ion, Nickel-Metal Hydride, and Lead-Acid batteries. LiPo was chosen as the power source due to its several advantages. It is lightweight, yet offers high capacity and energy density. The high discharge rate ensures quick power delivery to the thrusters [54]. Given the power requirements as well as the desired operation time (at least 1 hour), we selected the 6s, 14000 mAh, 25C from Tattu and the - 4S, 9600mAh, 130C battery from Hoova, for the propellers and electronics, respectively.

5.0.2 Instrumentation and Control

At the heart of our dual-USV platform, we adopt Cube Orange, which is originally developed for the UAV industry. This embedded system readily includes some of the required USV sensors, namely the Inertial Measurement Unit (IMU), barometers, and compasses, as well as access ports for CAN bus, serial ports, and I2C. The Cube Orange is preferred over its alternatives, such as Pixhawk, due to its redundant IMUs, and more number of serial, and CAN bus ports. It also allows for the addition of other sensors such as range finders, and companion computers for more complex processing tasks. Cube-Orange supports multiple GPS modules - serial as well as CAN-GPS modules such as Here 4 Multiband RTK, which is the preferred GPS for this project owing to its accuracy and multiband GNSS - enhancing

much needed reliability near buildings and trees. The GPS also uses the CAN bus port, hence leaving the existing serial ports available for other sensors. The Cube Orange can operate firmware such as Ardupilot[55] or PX4[56], both of which support actuator control for vehicle navigation. For our dual-USV platforms, we opted for the Ardupilot firmware due to our prior experience with it and its in-built obstacle avoidance capabilities.

5.0.3 Ground Station and Telemetry

To steer the USV and monitor its telemetry and health, a ground station is typically used. This comprises a software component running on a computer or tablet connected to the USV via radio at commonly available frequencies of 930MHz, 2.4GHz, or 5GHz. The latter frequencies are often used when streaming live camera feeds from the USV. The hardware further includes a remote controller. The software interface receives and displays telemetry information and camera feeds. Radio communications are generally limited to Line of Sight (LOS), although advanced systems may include signal repeaters placed in the field to ensure reliable communication with the USV. Repeaters are particularly beneficial in surveying operations around bridge columns, where direct LOS may be obstructed, enhancing the mission’s safety. We chose the SIYI MK32-HM30 Combo, a handheld ground station that integrates control and telemetry into a single Android tablet, has a long transmission range of 15 kilometers, dual camera feed capability, and is compatible with signal repeaters. On the software side of the ground station, two popular options are Mission Planner[57] and QGroundControl[58]. QGroundControl is a better choice for research due to its cross-platform support, built-in video streaming support and user-friendly interface.

5.0.4 Speed Controllers and Number of Propellers

The speed controller, also known as Electronic Speed Controller (ESC) receives PWM signals from the Cube-Orange and regulates the voltage input to the propeller. Based on our thrust estimation (section 4.1) we chose the Blue Robotics T500 propeller, along with the Hobbywing Quicrun WP 8BL150 G2 ESC. In general ESCs are chosen based on voltage, and current requirements of the thruster. It is important to ensure the selected ESC is capable of bidirectional motor control. As per T500 datasheet [52] the thruster has a max static (nominal) thrust of 16.44Kgf (161N) at 24V. When in motion, a $\eta_c = 0.5$ reduction is expected [59]. As noted before, we include a safety factor $k_s = 1.25$, leading to a final thrust of $T_f = 538.07N$ (see section 4.1). To achieve this, four T500 thrusters are needed.

5.0.5 Companion Computer

The Cube Orange is only compatible with simple sensory modalities such as range finders and support simple controllers such as PID. As a research platform, the dual-USV system should be able to accommodate more advanced sensors with higher data throughput, such as cameras and 3D LiDARs. It should also allow for the implementation of sophisticated control algorithms, image processing, machine learning, and other advanced computational tasks. For this purpose, the system is augmented with a companion computer. The companion computer can simultaneously access the Cube Orange to utilize its sensors (both embedded and external) while also interfacing with additional advanced sensors like cameras and LiDARs. Depending on the research requirements, the companion computer can either directly consume its collected sensory data e.g. through machine learning, or after additional processing and sensor fusion to extract ego or obstacle position/speed information, can relay the results to the Cube Orange for processing by its embedded controller. Furthermore, information from either Cube Orange or the companion computer may be relayed to the user for research and monitoring purposes. This integration allows us to leverage the companion computer’s flexibility and enhanced functionality on the USV while also benefiting from the fail-safe and already established, community-tested capabilities of the Cube Orange.

Given the potentials of machine learning in the control of autonomous mobile systems, we selected the Nvidia Jetson series for the companion computer due to its reasonably powerful GPU, suitable for real-time computer vision and other machine learning algorithms, and its energy-efficient design for embedded applications.

5.0.6 Sensors: Obstacle Detection and Range Estimation

For obstacle avoidance, sonar, and single-beam LiDARs can be natively connected to the Cube-Orange. Ardupilot supports a range of such sensors, and includes a few community-evaluated path-planning and obstacle-avoidance algorithms. As noted earlier, in addition to sensors that are natively supported on the Cube Orange, through the use of a companion computer more complex sensors such as stereo cameras or multibeam LiDARs can be used to provide 3D point cloud data, and detect and classify obstacles, etc. The companion computer can read/process more complex sensory data, and encapsulate processed results into Micro Air Vehicle Link (MAVLink) messages [60], which can then be received and processed by Ardupilot on the Cube Orange. Our proposed design uses the following sensors:

1. **Blue Robotics Ping 2 Sonar sensor:** This is an underwater sonar sensor, developed by Blue Robotics. Before integrating the sonar sensor into the USV, we conducted preliminary tests in a UC Davis pool. By collecting sensory data at different sensor angles, we evaluated its reliability and investigated how the mounting angle affects ground plane detection versus the identification of forward obstacles. A 20-degree mounting angle (with respect to the water surface) was found to provide a good balance, effectively detecting forward obstacles while also identifying shallow conditions that could cause the boat to become stuck in mud or collide with the waterbed which can damage the MBES. An angle larger than 50° was found to be more suitable for ground-plane detection. This sensor could be directly integrated with the cube orange. However, as discussed in the following, for sensor fusion when used in conjunction with other sensors, it is connected to the companion computer.
2. **Slamtec S3 LiDAR:** This sensor is IP-rated and features an ambient light anti-interference capability of up to 80,000 lux [61], ensuring reliable performance even in high-light environments, making it a suitable candidate for USV applications. This LiDAR is not natively supported by Ardupilot, and hence requires additional processing on the companion computer before encapsulating into MAVLink messages to the Cube Orange.

The selected LiDAR and sonar sensors are connected to the companion computer, where a script fuses their corresponding measurements into a 72 element array capturing 360° around the USV. This array is then packaged into Obstacle Distance message type of MAVLink, which is published to Ardupilot via the serial port providing a unified input that simultaneously covers obstacles above and below the water and can be used by either the obstacle avoidance algorithms available on Ardupilot or those custom implemented on the companion computer.

5.0.7 MultiBeam Echo Sounder

The BEP-USV is instrumented with a Norbit iWBMS MultiBeam Echo Sounder (MBES). This is a compact, high-resolution, broadband multibeam sonar system designed for bathymetric surveying. Aside from the size requirements, the MBES selection was driven by our budget limitations. Priced > \$120,000, this MBES system is on the lower end of the typical \$75k to \$500k range for commercially available systems. It is equipped with an advanced GNSS-aided inertial navigation system, and hence, is capable of position and roll stabilization, which enhances accuracy. This sonar operates at a center frequency of 400 kHz, with a frequency range of 200 to 700 kHz, and a ping rate of up to 60 Hz. Additional details can be found in the sensor datasheet [62].

An overview of the USV system architecture, along with the major components, and communication protocols is demonstrated in Fig. 9.

6 Control Strategies Available on the Companion Computer

In the rapidly evolving field of autonomous surface vehicles, the ability to develop, implement, and test diverse control systems is crucial for driving innovation and advancing research. Research in this domain often demand varying levels of interaction with vehicle dynamics, from low-level thrust control to high-level strategic navigation. By offering flexibility in control complexity, our platform supports a wide range of objectives, enabling researchers to focus on specific aspects of marine technology without needing to master every detail. This adaptability is particularly valuable in bathymetry, where requirements span from precise thrust control for obstacle avoidance and disturbance rejection to path planning for efficient data collection and environmental interaction. To address these needs, our USV platform allows for three distinct control strategies.

1) Direct Propeller Control: At the lowest level, our USV platform offers direct control over each propeller’s speed. This mode is needed for diving deep into the dynamics of the vessel, providing the granular control necessary for experiments focusing on propulsion, hydrodynamics, and low-level motion control affecting the USV’s robustness to external disturbances, stability, maneuverability, and efficiency. This option bypasses the Ardupilot’s internal control loops where each thruster is linked to a separate radio channel, managed by the companion computer. It also permits remote control takeover from the ground station when necessary. This configuration lacks built-in safety measures and, therefore, must be used with caution. Further details on these safety considerations are elaborated in our GitHub repository [53].

2) Velocity and Heading Control: Raising the level of abstraction, the second strategy enables researchers to control the USV’s velocity and heading without delving into the complexities of its hydrodynamics or the higher-order dynamics of the vessel and its propellers. This intermediate level of control is useful for the development of system agnostic, and generalizable approaches to navigation. It suits applications such as machine learning, where algorithms like reinforcement learning dictate the direction and speed of the boat, focusing on strategic decision-making for example in the presence of dynamic and static obstacles and high-flow disturbances [63]. It is particularly useful in fields such as

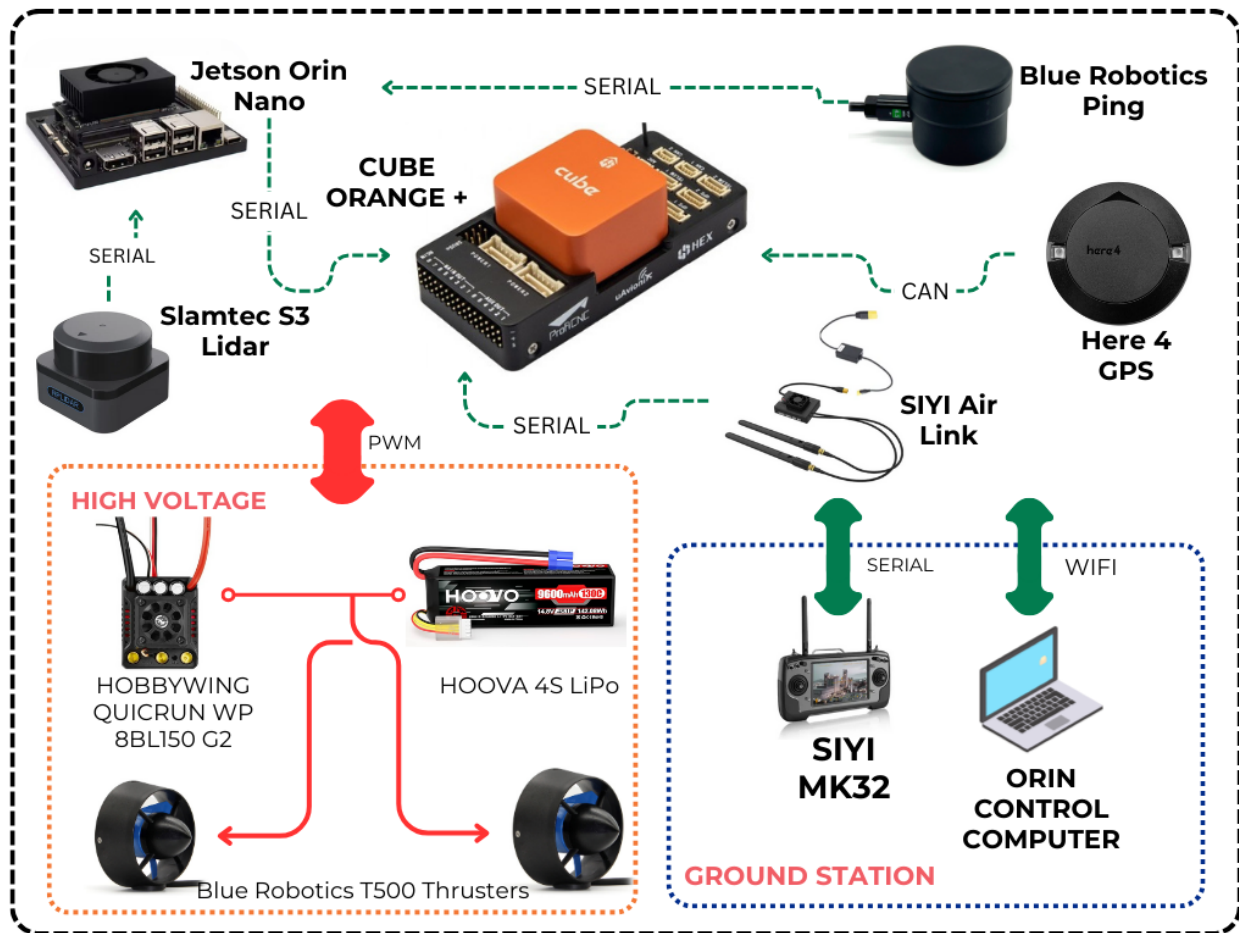


Figure 9: The Architecture of USV with its Components

computer science, where it's assumed that low-level control specifics can be adapted and optimized for each platform by dedicated specialists. In our implementation, this control mode involves the native PID controllers of the Ardupilot firmware.

3) Trajectory Control: The highest level of control abstracts all dynamics considerations, allowing the researcher to focus solely on the USV's position trajectory. This strategy, which relies on the GPS measurements, is essential for studies that prioritize path planning, static obstacle avoidance, or specific mission tasks such as bathymetric surveying where the primary concern is the geographic path of the vessel rather than the specifics of how it is achieved. By managing all underlying dynamics internally, this mode enables researchers to concentrate on developing path planning algorithms, e.g. for optimized data collection and processing. Much similar to the Velocity-Heading Control, this mode utilizes Ardupilot's native control to navigate along the provided trajectory.

To implement these three control strategies, we use various Ardupilot's operation modes and further leverage two critical tools, the MAVLink messaging protocol and the ROS2 publisher/subscriber model, as discussed in the following.

The Cube Orange has several operation modes available on Ardupilot: 1) Manual, 2) Guided, 3) Loiter, 4) Auto, and 5) Return To Launch (RTL). These modes provide different functionality and safety features. Under manual mode, the Helmsman commands the steering using their remote control (RC) where Ardupilot directly commands the thrusters based on the RC stick position. We leveraged this mode to implement Direct Propeller Control (strategy 1). Guided mode, leveraged for control strategies 2 and 3, allows real-time navigation of a USV using commands from the ground control station on the companion computer. It enables movement to specified positions, change heading, speed or dynamic re-tasking. There are 3 other modes available on ardupilot which may come handy under various circumstances: Loiter mode holds the USV in its last known location and heading and attempts to maintain that position under external disturbances. Auto mode allows for a pre-defined route to be sent from the ground station to the USV, which is then executed. This mode is particularly useful for conventional surveying missions and data collection. RTL

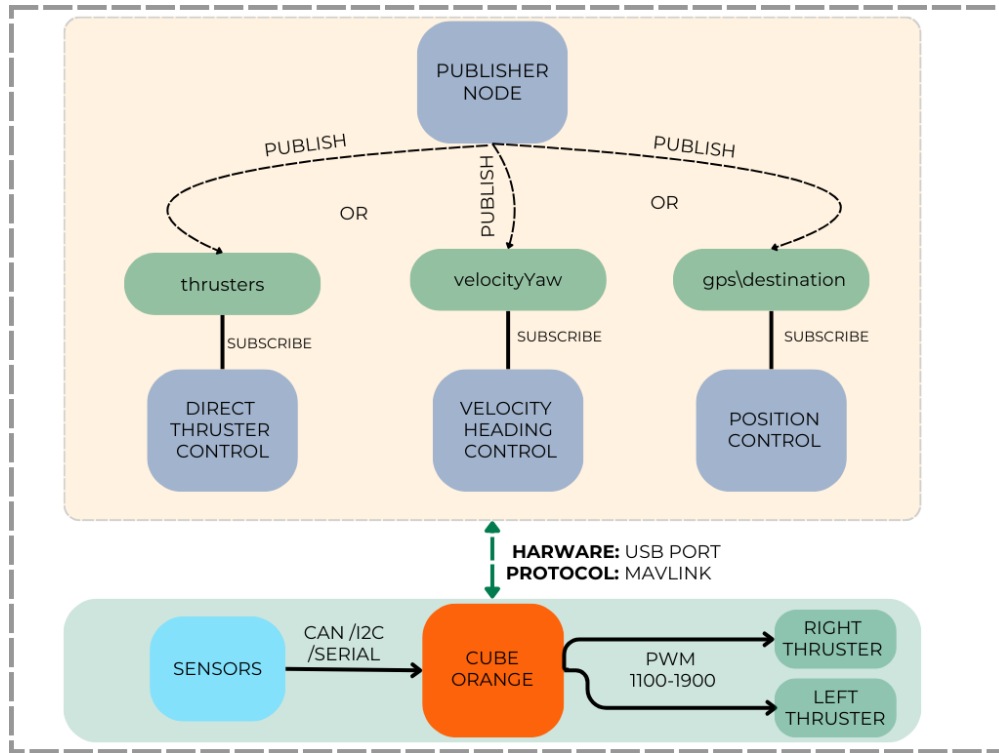


Figure 10: ROS2 Nodes with Ardupilot

brings the USV back to its departure position. In conjunction with these modes, Ardupilot features some fail-safe mechanisms such as RTL upon detection of low battery, arming checks to ensure availability of valid GPS/Compass readings, etc. These features are essential to the safe mission execution.

In addition to manual and guided modes, the MAVLink messaging protocol and the ROS2 publisher/subscriber model are used to implement the three distinct control strategies discussed above. Fig 10 outlines the ROS node architecture. It is noted that only one control strategy can be active at any given time.

MAVLink [60], a lightweight and standardized communication protocol used in the ArduPilot firmware, facilitates the exchange of information between the USV, the ground station, and the companion computers. This protocol is essential for transmitting navigation control and supports a range of commands including velocity and location directives. The MAVLink protocol’s capabilities are documented comprehensively in the official MAVLink repository [60].

In conjunction with MAVLink, we employ the Robotic Operating System 2 (ROS2-Humble) [64], which uses a publisher/subscriber model to facilitate component communication within robotic systems. In our setup, ROS2 is configured to publish MAVLink commands tailored to each of the three control strategies—direct thruster speed, velocity/heading, and trajectory control.

In our current implementation, publisher nodes await user-specified values, while a subscriber node connects and relays these values as MAVLink messages to the ArduPilot. Researchers can modify the publisher nodes and integrate their own code to tailor the system’s functionality to their specific needs. Detailed instructions for code modifications and setup are available in the GitHub Repo [53].

7 Experimental Evaluation

The control strategies discussed in section 6 were tested, and speed, and heading were recorded onboard using Ardupilot’s logging system. Table 4 lists the achieved top ground speeds for both NAC and BEP USVs along with their battery runtimes. At the time of testing, the river was relatively calm, so the ground speed and velocity relative to the water were expected to be similar. In our initial functionality tests, we used smaller, lower-voltage batteries on the NAC-USV than those installed on the BEP-USV 5.0.1 to simplify the NAC-USV setup. These batteries can be easily replaced as needed. Additionally, although our thrust estimation indicated a requirement for four T500 thrusters, we

Table 4: USV battery and runtimes.

Boat	Total Battery	Run Time	Top Speed
BEP-USV	22000 mAh – 6S × 3	3 Hours	2.2 m/s
NAC-USV	9600 mAh – 4S × 1	40 mins	1.8 m/s

initially deployed only two propellers to validate system functionality and reliability before incorporating additional thrusters. Consequently, the maximum speeds recorded during these tests were lower than our target speed, particularly for the NAC-USV due to its smaller batteries. The BEP-USV reached a top speed of 2.2 m/s with just two propellers, demonstrating that our desired speed (3.6 m/s) is attainable with the addition of two more propellers. The values reported for BEP-USV are taken during a bathymetry survey under non-flood conditions. Figure 11 presents an example bathymetry scan from the American River in Sacramento, illustrating a scour hole characterized by a sudden drop in underwater elevation.

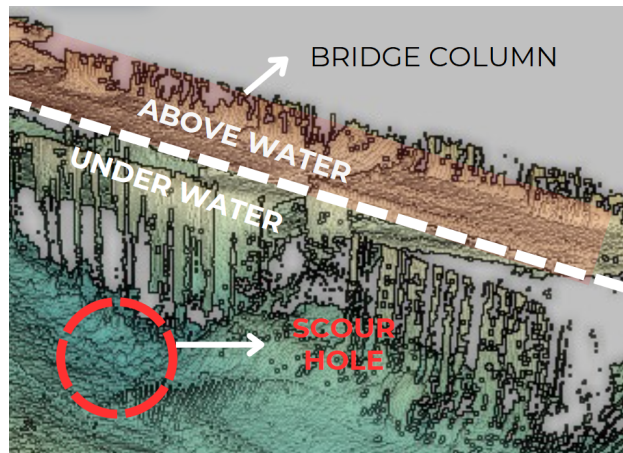


Figure 11: Bathymetry Data with scour hole detected

Direct Propeller Control: Tests on the NAC-USV demonstrated its ability to perform direct thruster control. While no quantifiable metrics are available for this control strategy, a video on the paper’s GitHub page [53] qualitatively

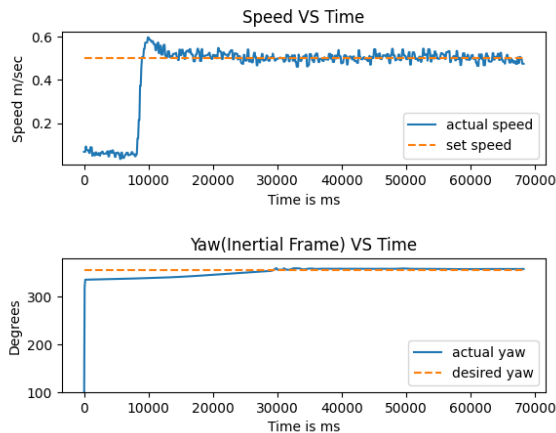


Figure 12: Speed 0.5 m/sec Heading 360°

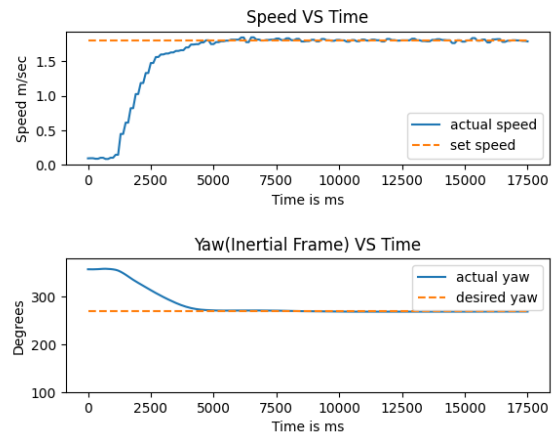


Figure 13: Speed 1.8 m/sec Heading 270°

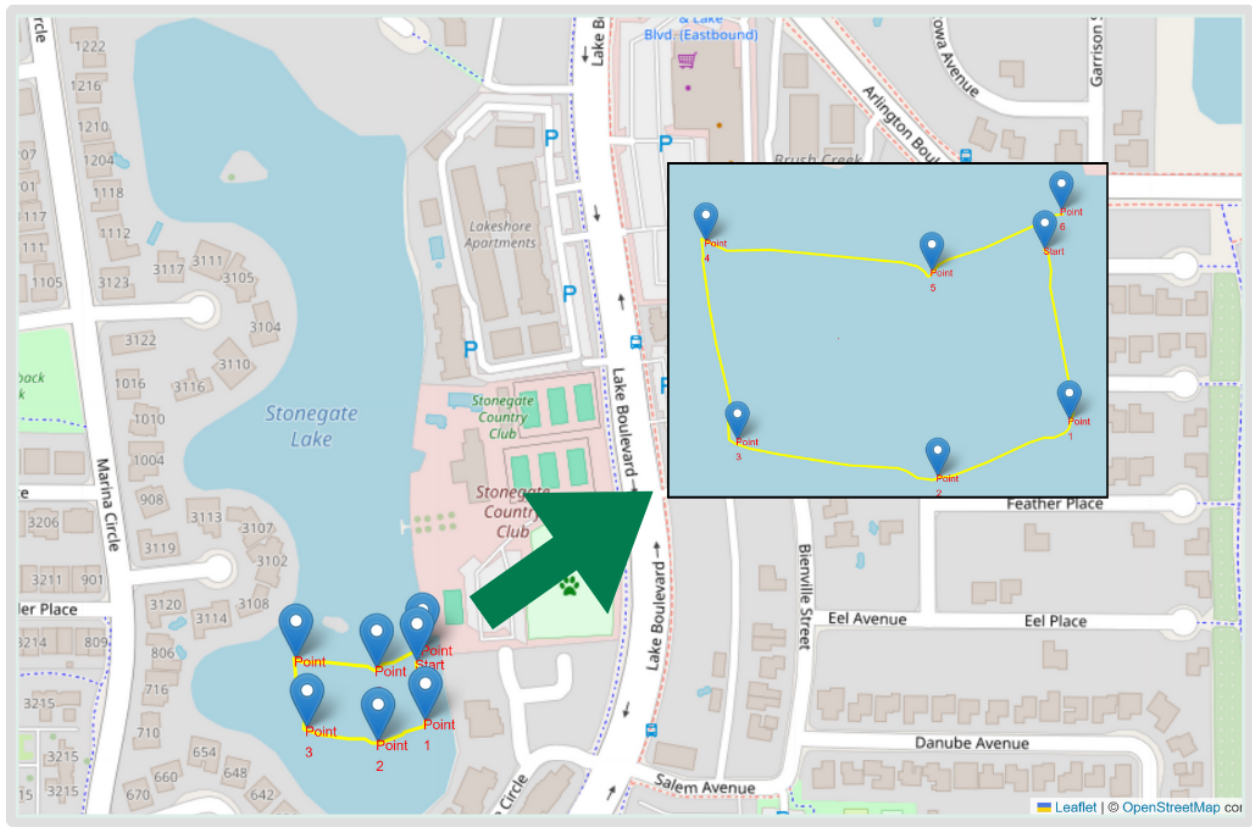


Figure 14: Position Control of USV [66]

showcases its performance using a Logitech G920 remote controller [65]. Since the control hardware on the NAC and BEP USVs are virtual replicas, the experiment was conducted exclusively on the NAC-USV system.

Velocity and Heading Control: Figs 12 and 13 show the NAC-USV's speed and heading response over time upon commanding the desired values. The USV achieves the commanded set points, thus validating that the system is capable of receiving and executing velocity and heading from the companion computer.

Trajectory Control: Fig 14 shows a sample executed multi-waypoint trajectory. The markers indicate the waypoints as commanded by the user to the NAC-USV. The node is set up such that upon reaching the target, the boat will enter into the loiter mode and attempts to stay within a 2-meter radius of the waypoint. This radius is a configurable parameter in Ardupilot. Waypoints can be overridden with a new waypoint at anytime to form a trajectory in realtime.

8 Conclusion and future work

This paper detailed the design and implementation of a dual USV system specifically tailored for bathymetry research under high-flow conditions. The two systems, namely the NAC-USV and BEP-USV, were developed to meet the needs of the research community, focusing on safe and adaptable approaches to control, navigation, data collection, and processing in uncrewed bathymetric operations.

The NAC-USV serves as a low-cost platform for developing and testing navigation and control technologies while minimizing the risk to expensive bathymetry equipment. The BEP-USV, a close replica of the NAC-USV with the addition of a high-resolution MBES, extends these tested capabilities to bathymetric surveying. As it mirrors the control systems and hardware configurations of the NAC-USV, the BEP-USV seamlessly integrates tested control and navigation frameworks directly from its NAC counterpart, enabling further research under safer and more predictable conditions.

As part of our system software architecture, we have developed and implemented three distinct control strategies tailored to meet the diverse needs of researchers. The first strategy enables direct control over each propeller, providing granular manipulation ideal for those delving into the complexities of advanced boat control and dynamics. The second strategy elevates the level of abstraction, allowing researchers to specify the USV's velocity and heading, thus catering to studies focused on navigation and dynamic obstacle avoidance without engaging with the details of the vessel's dynamics. The third strategy hides all the dynamic elements, concentrating solely on high-level strategic tasks such as bathymetry data collection and processing, trajectory optimization and static obstacle avoidance. This tiered approach ensures that our platform can support a wide range of research objectives, facilitating interdisciplinary studies and broadening the scope of potential applications.

By open-sourcing our platform and providing comprehensive documentation in the accompanying GitHub repository [53], we aim to empower the research community to build upon our work and drive innovation in bathymetry USV technology.

Acknowledgment

This work was supported by the California Department of Transportation (CALTRANS). We extend our appreciation to Hrushikesh Mathi, Kokul Aananth Kathiravan Kavitha, and James Chow who assisted with testing, validation and debugging. Map data is copyrighted by OpenStreetMap contributors and is available from <https://www.openstreetmap.org> [66].

References

- [1] Francesco Mugnai, Valentina Bonora, and Grazia Tucci. Integration, harmonization, and processing of geomatic data for bridge health assessment: the lastra a signa case study. *Applied Geomatics*, 15(3):533–550, 2023.
- [2] Quanbo Xin, Yajie Hu, and Kexin Bao. Spatial and temporal data analysis of waterway depth for preventive maintenance. In *2022 International Conference on Electronics and Devices, Computational Science (ICEDCS)*, pages 474–479. IEEE, 2022.
- [3] Tata Herbert, Nzelibe Ifechukwu Ogochukwu, and FA John. Bathymetric mapping for safe navigation: A case study of part of lagos lagoon. *Afr. Sch. J. Environ. Des. Constr. Mgt.(AJECM)*, 14:1–13, 2019.
- [4] Marco Reggiannini and Ovidio Salvetti. Seafloor analysis and understanding for underwater archeology. *Journal of Cultural Heritage*, 24:147–156, 2017.
- [5] David S Mueller and C Russell Wagner. Field observations and evaluations of streambed scour at bridges. Technical report, United States. Federal Highway Administration. Office of Research . . . , 2005.
- [6] Zhuoxiao Li, Zitian Peng, Zheng Zhang, Yijie Chu, Chenhang Xu, Shanliang Yao, Ángel F García-Fernández, Xiaohui Zhu, Yong Yue, Andrew Levers, et al. Exploring modern bathymetry: A comprehensive review of data acquisition devices, model accuracy, and interpolation techniques for enhanced underwater mapping. *Frontiers in Marine Science*, 10:1178845, 2023.
- [7] Anne-Cathrin Wölfl, Helen Snaith, Sam Amirebrahimi, Colin W Devey, Boris Dorschel, Vicki Ferrini, Veerle Al Huvenne, Martin Jakobsson, Jennifer Jencks, Gordon Johnston, et al. Seafloor mapping—the challenge of a truly global ocean bathymetry. *Frontiers in Marine Science*, 6:434383, 2019.
- [8] Radoslaw Guzinski, Elias Spondylis, Myrto Michalis, Sebastiano Tusa, Giacomina Brancato, Lorenzo Minno, and Lars Boye Hansen. Exploring the utility of bathymetry maps derived with multispectral satellite observations in the field of underwater archaeology. *Open Archaeology*, 2(1), 2016.
- [9] S Fleming, T Jordan, M Madden, EL Usery, and R Welch. Gis applications for military operations in coastal zones. *ISPRS Journal of Photogrammetry and Remote Sensing*, 64(2):213–222, 2009.
- [10] Shuai Teng, Airong Liu, Xijun Ye, Jialin Wang, Jiyang Fu, Zhihua Wu, Bingcong Chen, Chao Liu, Haoxiang Zhou, Yuxin Zeng, et al. Review of intelligent detection and health assessment of underwater structures. *Engineering Structures*, 308:117958, 2024.
- [11] Kris EJ Campbell, Alastair Ruffell, Jamie Pringle, David Hughes, Su Taylor, and Brian Devlin. Bridge foundation river scour and infill characterisation using water-penetrating radar. *Remote Sensing*, 13(13):2542, 2021.
- [12] WRGB CBS6 Albany. 35 years ago: 10 died in schoharie thruway bridge collapse. <https://cbs6albany.com/news/local/35-years-ago-10-died-in-schoharie-thruway-bridge-collapse>. Accessed: 2025-01-17.

- [13] Mohamed Zaid, Zeinab Yazdanfar, Harun Chowdhury, and Firoz Alam. A review on the methods used to reduce the scouring effect of bridge pier. *Energy Procedia*, 160:45–50, 2019. 2nd International Conference on Energy and Power, ICEP2018, 13–15 December 2018, Sydney, Australia.
- [14] M.L. Seto and A. Crawford. Autonomous shallow water bathymetric measurements for environmental assessment and safe navigation using usvs. In *OCEANS 2015 - MTS/IEEE Washington*, pages 1–5, 2015.
- [15] Andre Godin. *The Calibration of Shallow Water Multibeam Echo-Sounding systems*. PhD thesis, University of New Brunswick, 1996.
- [16] Subrata K. Chakrabarti. Chapter 3 - ocean environment. pages 79–131, 2005.
- [17] Zhewen Xing, Youmin Zhang, and Chun-Yi Su. Active wind rejection control for a quadrotor uav against unknown winds. *IEEE Transactions on Aerospace and Electronic Systems*, 59(6):8956–8968, 2023.
- [18] Bo Dai, Yuqing He, Guangyu Zhang, Feng Gu, Liying Yang, and Weiliang Xu. Wind disturbance rejection for unmanned aerial vehicle based on acceleration feedback method. In *2018 IEEE Conference on Decision and Control (CDC)*, pages 4680–4686, 2018.
- [19] Arthur P. Mendez, James F. Whidborne, and Lejun Chen. Experimental verification of an lidar based gust rejection system for a quadrotor uav. In *2022 International Conference on Unmanned Aircraft Systems (ICUAS)*, pages 1455–1464, 2022.
- [20] Alejandro Gonzalez-Garcia, Herman Castañeda, and Leonardo Garrido. Usv path-following control based on deep reinforcement learning and adaptive control. In *Global Oceans 2020: Singapore – U.S. Gulf Coast*, pages 1–7, 2020.
- [21] Meng Joo Er, Chuang Ma, Tianhe Liu, and Huibin Gong. Intelligent motion control of unmanned surface vehicles: A critical review. *Ocean Engineering*, 280:114562, 2023.
- [22] Michael Benjamin, Joseph Curcio, John Leonard, and Paul Newman. Protocol-based colregs collision avoidance navigation between unmanned marine surface craft. *Journal of Field Robotics*, 23(5):333–346, 2006.
- [23] Jianwen Li, Jalil Chavez-Galaviz, Kamyar Azzadenesheli, and Nina Mahmoudian. Dynamic obstacle avoidance for usvs using cross-domain deep reinforcement learning and neural network model predictive controller. *Sensors*, 23(7), 2023.
- [24] Kaiwen Xue, Jiawei Liu, Nan Xiao, Xiaoqiang Ji, and Huihuan Qian. Underwater and surface obstacle detection with stereo vision method for usv collision avoidance risk assessment in shallow water.
- [25] Ma Teng, Li Ye, Zhao Yuxin, Jiang Yanqing, Zhang Qianyi, and António M. Pascoal. Efficient bathymetric slam with invalid loop closure identification. *IEEE/ASME Transactions on Mechatronics*, 26(5):2570–2580, 2021.
- [26] Jiarui Tan, Ignacio Torroba, Yiping Xie, and John Folkesson. Data-driven loop closure detection in bathymetric point clouds for underwater slam. In *2023 IEEE International Conference on Robotics and Automation (ICRA)*, pages 3131–3137, 2023.
- [27] Kimdu. Mil-std-461 vs mil-std-810: Understanding the difference. <https://kimdu.com/mil-std-461-vs-mil-std-810-understanding-the-difference/>. Accessed: 2025-01-22.
- [28] C. J. Legleiter and P. J. Kinzel. Improving remotely sensed river bathymetry by image-averaging. *Water Resources Research*, 57(3):e2020WR028795, 2021. e2020WR028795 2020WR028795.
- [29] Julian Deunf, Nathalie Debese, Thierry Schmitt, and Romain Billot. A review of data cleaning approaches in a hydrographic framework with a focus on bathymetric multibeam echosounder datasets. *Geosciences*, 10, 07 2020.
- [30] Zhuoxiao Li, Zitian Peng, Zheng Zhang, Yijie Chu, Chenhang Xu, Shanliang Yao, Ángel F. García-Fernández, Xiaohui Zhu, Yong Yue, Andrew Levers, Jie Zhang, and Jieming Ma. Exploring modern bathymetry: A comprehensive review of data acquisition devices, model accuracy, and interpolation techniques for enhanced underwater mapping. *Frontiers in Marine Science*, 10, 2023.
- [31] Daniel F. Carlson, Alexander Fürsterling, Lasse Vesterled, Mathias Skovby, Simon Sejer Pedersen, Claus Melvad, and Søren Rysgaard. An affordable and portable autonomous surface vehicle with obstacle avoidance for coastal ocean monitoring. *HardwareX*, 5:e00059, 2019.
- [32] Gerben Peeters, Marcus Kotzé, Muhammad Raheel Afzal, Tim Catoor, Senne Van Baelen, Patrick Geenen, Maarten Vanierschot, René Boonen, and Peter Slaets. An unmanned inland cargo vessel: Design, build, and experiments. *Ocean Engineering*, 201:107056, 2020.
- [33] Dina Khaled, Hussien Aly, Mariam Khaled, Nourhan Mahmoud, Sameh Shabaan, and Ahmed Abdellatif. Development of a sustainable unmanned surface vehicle (usv) for search and rescue operations. In *The International Undergraduate Research Conference*, volume 5, pages 462–468. The Military Technical College, 2021.

- [34] Joga Dharma Setiawan, Muhammad Aldi Septiawan, Mochammad Ariyanto, Wahyu Caesarendra, M Munadi, Sabri Alimi, and Maciej Sulowicz. Development and performance measurement of an affordable unmanned surface vehicle (usv). *Automation*, 3(1):27–46, 2022.
- [35] Mohamad Hazwan Mohd Ghazali, Mohd Hafiz Abdul Satar, and Wan Rahiman. Unmanned surface vehicles: From a hull design perspective. *Ocean Engineering*, 312:118977, 2024.
- [36] Boater Exam. Boat hull types and designs. <https://www.boaterexam.com/boating-resources/boat-hull-types-designs/>. Accessed: 2025-01-16.
- [37] Drive a Boat Canada. Types of hulls. <https://driveaboatcanada.ca/types-of-hulls/>. Accessed: 2025-01-16.
- [38] 411 Marine. V-hull tag archive. <https://www.411marine.com/tag/v-hull/>. Accessed: 2025-01-17.
- [39] Muwanika Jdiobe. *Design and Development of a Water Observatory: An Autonomous Environmental Sampling System for In-Situ Sensing of Lakes and Rivers*. PhD thesis, Oklahoma State University, 2020.
- [40] United states naval academy, lecture notes: Principles of ship performance or engineering in the littoral zone or introduction to aeronautics.
- [41] J. Holtrop. A statistical analysis of performance test results. *International Shipbuilding Progress*, 24(270):23–28, 1977.
- [42] Nautilus Shipping. Form coefficient of ship. <https://www.nautilusshipping.com/form-coefficient-of-ship>. Accessed: 2024-10-25.
- [43] Keith Alexander. Waterjet versus propeller engine matching characteristics. *Naval engineers journal*, 107(3):129–139, 1995.
- [44] Chunyue Li, Jiajia Jiang, Fajie Duan, Wei Liu, Xianquan Wang, Lingran Bu, Zhongbo Sun, and Guoliang Yang. Modeling and experimental testing of an unmanned surface vehicle with rudderless double thrusters. *Sensors*, 19(9), 2019.
- [45] Kantapon Tanakitkorn and Surasak Phoemsapthawee. Impacts of thruster configurations on the task performance of an unmanned surface vehicle. *Ocean Engineering*, 256:111465, 2022.
- [46] R Vijayanandh, K Venkatesan, R Raj Kumar, M Senthil Kumar, G Raj Kumar, and P Jagadeeshwaran. Theoretical and numerical analyses on propulsive efficiency of unmanned aquatic vehicle’s propeller. In *Journal of Physics: Conference Series*, volume 1504, page 012004. IOP Publishing, 2020.
- [47] Car and Driver. How long is a long bed truck? <https://www.caranddriver.com/research/a32811097/how-long-is-a-long-bed-truck/>. Accessed: 2024-12-01.
- [48] Occupational Safety and Health Administration (OSHA). Standard interpretations - use of the revised niosh lifting equation. <https://www.osha.gov/laws-regs/standardinterpretations/2013-06-04-0>. Accessed: 2024-12-01.
- [49] California Data Exchange Center (CDEC). River conditions. <https://cdec.water.ca.gov/river/rivcond.html>. Accessed: 2025-01-22.
- [50] Mariusz Specht. Methodology for performing bathymetric and photogrammetric measurements using uav and usv vehicles in the coastal zone. *Remote Sensing*, 16(17), 2024.
- [51] Inc. Seafloor Systems. Seafloor systems. <https://www.seaflorsystems.com/>. Accessed: 2025-01-19.
- [52] Blue Robotics. T500 thruster. <https://bluerobotics.com/store/thrusters/t100-t200-thrusters/t500-thruster/>. Accessed: 2024-10-26.
- [53] Soltanilara. Arduboot-ros2. <https://github.com/Soltanilara/Twin-USV>. GitHub repository, accessed: 2025-01-17.
- [54] Mathilde Lacombe. 11 advantages of lipo batteries: Why you should consider using them. <https://mathildelacombe.com/11-advantages-of-lipo-batteries-why-you-should-consider-using-them/>. Accessed: 2025-01-17.
- [55] ArduPilot. Ardupilot documentation. <https://ardupilot.org>. Accessed: 2024-10-12.
- [56] a Linux Foundation project PX4 Autopilot, hosted by Dronecode. Px4 autopilot documentation. <https://px4.io>. Accessed: 2024-10-12.
- [57] ArduPilot. Mission planner documentation. <https://ardupilot.org/planner/docs/mission-planner-overview.html>. Accessed: 2024-10-12.

- [58] QGroundControl. Qgroundcontrol documentation. <https://docs.qgroundcontrol.com>. Accessed: 2024-10-12.
- [59] Yoshitaka Furukawa and Katsuro Kijima. Influence of forward speed on the thruster performance used on dynamic positioning system of offshore platform. *Transactions of the West-Japan Society of Naval Architects*, 85, 1993.
- [60] a Linux Foundation project MAVLink, hosted by Dronecode. Mavlink developer guide. <https://mavlink.io/en/>. Accessed: 2024-10-12.
- [61] Slamtec. Slamtec s3 lidar sensor. <https://www.slamtec.com/en/S3>. Accessed: 2025-02-05.
- [62] NORBIT Subsea. Norbit iwbps product sheet. https://norbit.com/media/PS-120006-23_iWBMS_Pn_12004_AACDB4_A4.pdf. Accessed: 2024-10-30.
- [63] Ehsan Kazemi and Iman Soltani. Marineformer: A spatio-temporal attention model for usv navigation in dynamic marine environments, 2024.
- [64] Open Robotics. Robot operating system (ros2) documentation. <https://docs.ros.org/en/humble>. Accessed: 2024-10-12.
- [65] Logitech. Logitech g920 driving force racing wheel user guide. <https://www.logitech.com/assets/53756/g920-driving-force-racing-wheel.pdf>. Accessed: 2024-10-12.
- [66] OpenStreetMap contributors. Planet dump retrieved from <https://planet.osm.org> . <https://www.openstreetmap.org>, 2017. Accessed: 2025-02-03.